

Final Report

for the research project entitled

Forecast Model Applications of Satellite-derived Cloud Parameters

submitted to

Dr. Scott Sandgathe
Program Director, Office of Naval Research

for the performance period covering
1 May 1998 - 30 October 2000

Contract # N00014-98-1-0556

Principal Investigators

Dr. Melanie Wetzel and Dr. Steven Chai
Division of Atmospheric Sciences
Desert Research Institute
University and Community College System of Nevada

1 December 2000

DISTRIBUTION STATEMENT A
Approved for Public Release
Distribution Unlimited

DTIC QUALITY INSPECTED 4
20001214 049



Dr. Scott Sandgathe
Marine Meteorology and Atmospheric Effects
Ocean, Atmosphere and Space Department
Office of Naval Research
800 North Quincy Street
Ballston Tower One
Arlington, VA 22217-5660

1 December 2000

Dear Dr. Sandgathe:

Enclosed please find three copies of the final report for the ONR-DEPSCoR contract N00014-98-1-0556, "Forecast Model Applications of Satellite-derived Cloud Parameters". Participating in the ONR research program has been scientifically rewarding and has led to new avenues of study within DRI and in conjunction with the Naval Research Laboratory in Monterey. I very much appreciate the guidance and support which you have generously provided during the project.

Sincerely yours,

A handwritten signature in cursive script that appears to read "Melanie A. Wetzel".

Melanie A. Wetzel, Ph.D.
Associate Research Professor
Division of Atmospheric Sciences
Desert Research Institute

Email: wetzel@dri.edu

Copies : DTIC (2) ✓



Project Summary

Development of satellite remote sensing retrieval methods, numerical model studies and field observational research have been conducted to advance the use of cloud physical parameters with the Navy's Coupled Ocean/Atmosphere Mesoscale Prediction System (COAMPS) prediction model. Procedures have been demonstrated for the satellite retrieval techniques and the merging of these retrieved parameters with COAMPS model output.

A field research project was planned and carried out in conjunction with scientists from the Naval Research Laboratory, the University of Wyoming and Oregon State University. This project took place during 4 August - 4 September 1999 in the region of coastal Oregon, and provided detailed study of COAMPS model forecasts using satellite multispectral data and instrumented aircraft observations. GOES satellite multi-channel data were used to develop an operational procedure for mapping parameters such as cloud optical depth, droplet effective radius and liquid water path. Aircraft measurements by the University of Wyoming King Air allowed *in situ* verification of the satellite retrieval parameters and of the forecast model simulations produced by the Navy's nonhydrostatic mesoscale prediction system, COAMPS. Case studies show that the satellite retrieval methods are valid, and demonstrate how the gridded cloud parameters retrieved from satellite data can be combined with model output to improve stratus nowcasting and forecasting.

Valuable new collaborative research was initiated and is continuing from this project. During the course of the project, six research meetings have been held (primarily at NRL-Monterey) with participation by NRL, the Desert Research Institute, the University of Wyoming, the Naval Postgraduate School, and Oregon State University. A six-month no-cost extension (1 May - 30 October 2000) was requested and granted for the project in order to complete the analysis of data obtained during the August 1999 field program. The research has resulted in a conference paper (Wetzel *et al.*, 2000a) and an article submitted to the AMS journal *Weather and Forecasting* (Wetzel *et al.*, 2000b).

1.0 Introduction

Prediction of boundary layer cloudiness is a critical but difficult aspect of marine forecasting, due to the mesoscale variability of boundary layer dynamic processes and the lack of observations in many oceanic and coastal regions. The ability to correctly simulate and forecast cloud layer evolution is strongly tied to the accuracy with which a model represents the evolution of the cloud profile of liquid water. This is due to the controlling influences of entrainment, turbulent mixing, radiative heating and microphysical processes within stratus decks.

Multichannel satellite remote sensing can provide near-continuous mapping of the distribution of stratus cloud layers (Lee *et al.*, 1997; Greenwald and Christopher, 2000), and can also be used to estimate physical parameters of the cloud such as effective droplet size, cloud optical depth and cloud liquid water path. Thus, satellite data offer a source of global and frequent source of validation data for marine cloud liquid water path distributions as forecast by COAMPS. There are several applications of this methodology such as improvement in short term forecasting, creation of cloud climatologies, and estimation of electromagnetic propagation. It is also anticipated that the satellite remote sensing of cloud microphysical parameters will be used in future versions of COAMPS which incorporate explicit prognostic routines and/or parameterizations for cloud droplet size.

2. 0 Project Results

2.1 Development of Remote Sensing Retrieval Methods

Multispectral satellite data for both sun-synchronous and geosynchronous platforms have been used to develop methods for combined analysis of cloud microphysical parameters with the Navy's COAMPS forecast model simulation results. Remote sensing retrieval methods previously demonstrated (Wetzel *et al.* 1996; Wetzel and Stowe, 1999) for satellite estimation of stratiform cloud droplet size and optical depth were implemented and adapted for the region and time period of study.

Satellite data are utilized from the NOAA polar-orbiter Advanced Very High Resolution Radiometer (AVHRR) sensor and the GOES geostationary Imager sensor. The primary channels used are the visible Channel 1 (0.57-0.72 μm on Imager and AVHRR) ; near-infrared, Channel 2 on Imager (3.78-4.03 μm), and AVHRR Channel 3 (3.55-3.93 μm) and the thermal infrared windows, Channel 4 (10.2-11.2 μm on Imager, and 10.3-11.3 μm on AVHRR) and Channel 5 (11.5-12.5 μm on Imager, 11.4-12.4 or 11.5-12.5 μm on AVHRR).

The Discrete Ordinates model (Stamnes *et al.*, 1988) was adapted to generate tabular data for multiple cloud droplet size, cloud optical depth and solar/viewing geometry conditions, covering the ranges of possible image passes and cloud types for summertime coastal stratus. The Streamer software package (Meier *et al.*, 1997) is a UNIX-based program which applies the Discrete Ordinates Model with gaseous absorption and aerosol extinction effects, and this was implemented for the satellite channels and stratus cloud characteristics simulated for this study. Use of this radiative transfer method has demonstrated the influence of aerosol on marine stratus cloud droplet size (Borys *et al.*, 1998).

Cloud-covered pixels were selected using channel threshold tests, and cloud optical depth and cloud droplet size are found by interpolation from the observed satellite pixel reflectances in the visible and near-infrared channels to the arrays of pre-calculated radiative transfer model reflectances. Model-calculated reflectance in the satellite visible channel is directly related to optical depth for the range of microphysical conditions observed in stratus cloud, so that satellite-observed reflected radiance can be directly used with model-calculated reflectances to retrieve cloud optical depth (Platnick and Valero, 1995). Figure 1 presents an example of the relationship between visible reflectance and cloud optical depth (τ) for a range of relative sun-satellite azimuth angles.

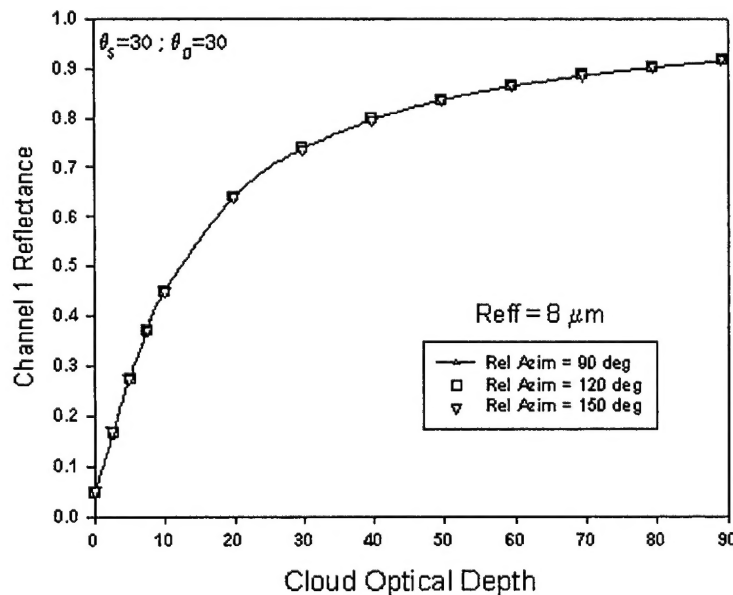


Fig 1. AVHRR Channel 1 reflectance calculated using the Discrete Ordinates radiative transfer model for stratus cloud of increasing optical depth, at three values of the sun-satellite relative azimuth angle (φ), the indicated conditions of satellite zenith angle (θ_s) and solar zenith angle (θ_0), and with cloud droplet effective radius (R_{eff}) of 8 μm .

The near-infrared reflectance obtained from the GOES Imager Channel 2 or the AVHRR Channel 3 decreases significantly as cloud droplet size increases, such that results for the range of sun-satellite viewing angles, cloud optical depth and droplet size can be utilized with observed satellite radiances to estimate droplet size. This relationship is most robust for the size distribution parameter known as the effective radius (typically denoted as R_e or R_{eff}), which is defined as the ratio of the volume-weighted and area-weighted integrals of the distribution, $n(r)$, of droplet radius, r ,

$$R_{\text{eff}} = \frac{\int_0^{\infty} r^3 n(r) dr}{\int_0^{\infty} r^2 n(r) dr}$$

Figure 2 presents an example of the cloud near-infrared reflectance in the AVHRR Channel 3 as droplet size increases. The thermal emission contribution to near-infrared radiance is removed by using the thermal infrared brightness temperature and an initial estimate of near-infrared emissivity for the cloud. The blackbody temperature is inverted to calculate the near-infrared blackbody radiance, and this is subtracted from the satellite-observed near-infrared radiance to obtain the near-infrared reflectance.

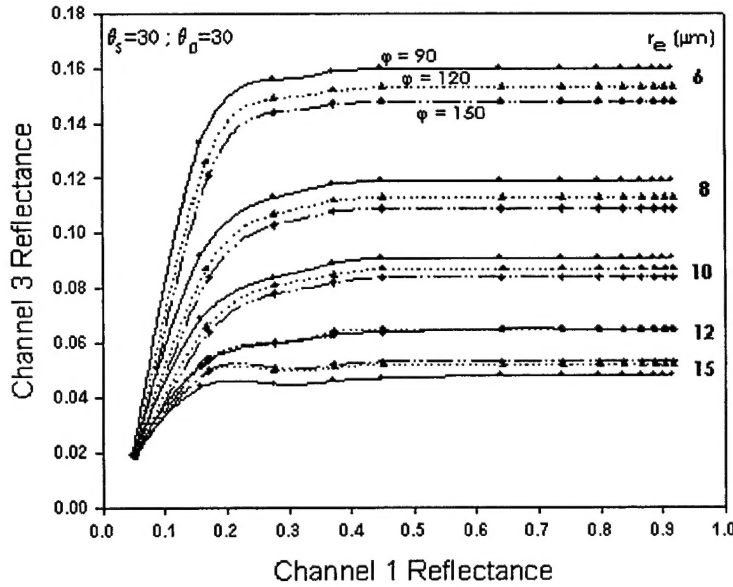


Fig. 2. AVHRR Channel 3 and Channel 1 reflectance curves calculated using the Discrete Ordinate model for a family of cloud layers with droplet effective radius increasing from 6 to 15 μm , at three different sun-satellite relative azimuth angles (ϕ) and the indicated conditions of satellite zenith angle (θ_s) and solar zenith angle (θ_0).

Cubic spline interpolation was implemented to first estimate cloud optical depth from visible reflectances, then to retrieve cloud droplet effective radius from the near-infrared reflectances for each cloudy pixel. The thermal infrared channel data were used to subtract the thermal emission component from the near-infrared radiance. The Discrete Ordinates model (Stamnes *et al.*, 1988; Meier *et al.*, 1997) was used to produce tabular data for a wide range of R_E , τ and solar/viewing geometry conditions.

A parameterization based on retrieved optical depth and effective droplet size (Stephens, 1978) provides the estimate of cloud liquid water path: $LWP = (2/3) \tau R_E$, where LWP has units (g m^{-2}), τ is non-dimensional, and R_E is in microns. Fig. 3 shows a comparison between the value of cloud liquid water path for cloud layers prescribed for the radiative transfer (RT) calculations, and the parameterized value as obtained from the equation above. The values of optical depth and effective radius used to calculate the parameterized LWP were determined from the RT model input conditions. Strong correspondence between the prescribed and parameterized values suggests satellite-estimated values of cloud optical depth and droplet effective radius can be used to estimate cloud liquid water path. Since liquid water path is a variable that is directly forecast by the COAMPS model, intercomparisons between the mapped distributions of satellite-derived and model-derived LWP can be evaluated. This retrieval method was tested first on datasets from the COAST '96 field measurement program for coastal stratus along California, and then implemented in a more detailed analysis for coastal cloud offshore Oregon during the COSAT '99 experiment.

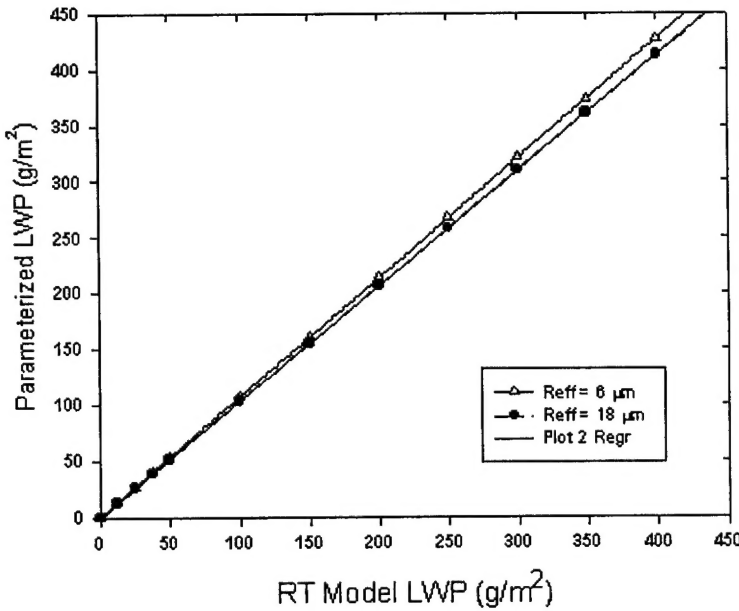


Fig. 3. Comparison of parameterized and model-prescribed stratus layer liquid water path (LWP).

3.0 COSAT '99 Project

3.1 Description of Field Measurements and Satellite Remote Sensing

The COSAT '99 field program was designed to implement and test the satellite remote sensing methods for use in COAMPS model validation and forecast evaluation. Aircraft measurements obtained by the UW King Air (Vali *et al.*, 1998) were utilized for detailed analysis of cloud structure as well as the vertical profiles of cloud droplet size and liquid water content. Multiple sensor systems recorded 1-Hz (and higher frequency) thermodynamic, air motion and microphysical parameters. The PMS FSSP, Gerber PVM, and DMT LWC-100 probes operated on the aircraft provided liquid water content and droplet size data for use in the intercomparisons with model and satellite-derived estimates. In addition, the King Air high-resolution Doppler radar allowed interpretation of the fine-scale structure of reflectivity and velocity characteristics within the cloud and boundary layer.

Summary data for aircraft parameters such as cloud R_e , liquid water content and temperature were selected from ascent/descent flight legs as well as constant-altitude segments in order to evaluate the vertical profiles and horizontal structure of the cloud layers. Case study datasets were obtained for 19 different aircraft sampling flights during the August 1999 field project. Examples will be presented here from a subset of these flight periods, selected due to the availability of simultaneous satellite and aircraft

datasets. Figure 4 is the visible GOES image and Figure 5 shows the corresponding R_e distribution at 1630 UTC on 17 August 1999. The short graphic overlay in Figure 5 is an example of the brief sub-segments from individual flight days that were used for the aircraft-satellite intercomparisons. Figure 6 presents the corresponding LWP distribution.



Fig. 4. GOES visible image at 1630 UTC, 17 August 1999, with graphic overlays of the flight track (red), latitude/longitude grid (blue), and Oregon coastline (green).



Fig. 5. GOES-derived cloud droplet effective radius (microns) at 1630 UTC, 17 August 1999, with graphic overlays of a segment of the flight track (red) and central Oregon coastline (white).

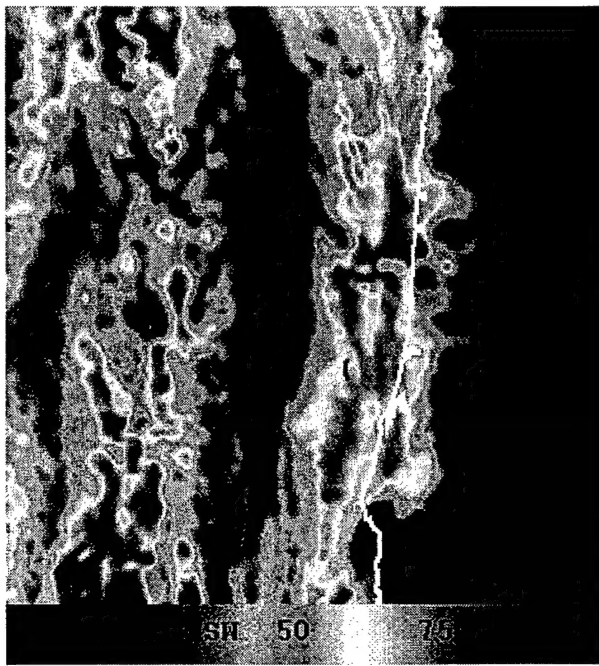


Fig. 6. GOES-derived cloud liquid water path (g m^{-2}) at 1630 UTC, 17 August 1999, with graphic overlays of a segment of the flight track (red) and central Oregon coastline (white).

Figure 7 portrays the vertical profiles of cloud liquid water content and effective radius for three rapid ascent and descent flight segments obtained during 1631-1634 UTC on 17 August. In this comparison, the measured LWP is 80 g m^{-2} , while the maximum LWP for the satellite image pixels along the flight segment is 65 g m^{-2} . The aircraft FSSP data and the satellite retrieval method indicated an effective radius value of $13 \mu\text{m}$. A series of similar intercomparisons were analyzed for several image dates and times. Individual flight segments are directly matched by geographic location to the gridded and mapped satellite retrieval parameters for the closest available satellite image dataset (within 15 minutes). Aircraft and satellite-derived values of effective radius and liquid water path for several flight segments are summarized in Table 1. This summary indicates agreement between aircraft measurements and the satellite-estimated parameters.

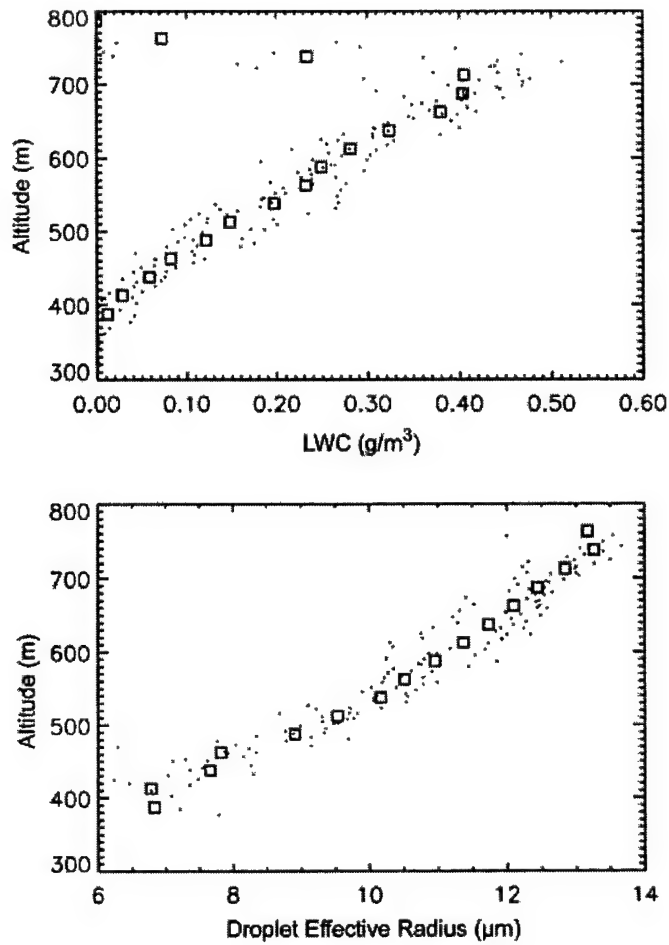


Fig. 7. Liquid water content (upper panel) and droplet effective radius (lower panel) from aircraft soundings on 17 August 1999 over the time period 16:31-16:34 UTC. Individual data points shown are 1-sec averages while the larger squares indicated averages of all data at 25-m height intervals. Data are derived from the King Air FSSP probe.

Table 1. Aircraft and satellite-derived values of maximum values of effective radius (R_e) and liquid water path (LWP), obtained from all measurement data within individual ascent/descent profiles.

Date / Time (UTC)	KingAir R_e (μm)	GOES R_e (μm)	KingAir LWP (g m^{-2})	GOES LWP (g m^{-2})
9 Aug / 1700	9	9	40	30
9 Aug / 1800	10	9	75	65
10 Aug / 1600	10	11	95	65
10 Aug / 1800	10	10	70	90
11 Aug / 1600	15	16	70	75
11 Aug / 1700	14	14	40	40
16 Aug / 1630	14	12	80	45
16 Aug / 1730	14	12	50	45
17 Aug / 1600	10	10	25	25
17 Aug / 1630	13	13	80	65

Variability in satellite-derived values of R_e along the aircraft sampling track during the profile data collection segments is $\leq 2 \mu\text{m}$, as is the variation in R_e typically observed by the aircraft in the top 50-100 m of the cloud layers. The differences between the satellite and aircraft values of R_e is within the range of differences noted for two independent droplet size probe systems that were operated on the aircraft (Gerber PVM and PMS FSSP). Sensitivity tests on calculated reflectances for stratus clouds with vertically increasing droplet size (Wetzel and Vonder Haar, 1991) indicate that for the conditions of R_e and liquid water content profiles described here, the satellite-estimated R_e represents the actual R_e in the top 100 meters of cloud to an accuracy of 1-2 μm .

Estimates of cloud liquid water path were obtained from the parameterization of satellite-retrieved cloud optical depth and effective droplet radius, and mapped over the satellite image domain. The summary of LWP intercomparisons shown in Table 1 shows a similar range of differences between aircraft and satellite values (up to 35 g m^{-2}) as the range of variation in satellite-estimated LWP along individual sampled flight segments (up to 25 g m^{-2}).

The values shown in Table 1 are from different locations, sampling different portions of the cloud zone, so temporal differences on a given day or between days do not indicate overall trends. The magnitudes of aircraft and satellite estimates of R_e and LWP are similar to those obtained for observational studies of California coastal stratus summarized for the FIRE-Stratus characterization program (Minnis et al., 1992). Intercomparison of the satellite and aircraft results for the COSAT '99 cases suggests a possible bias toward satellite underestimation of LWP. Since a comparable tendency is not seen in the comparisons of estimated and *in situ* droplet size, a bias in retrieved LWP estimates in those cases can be attributed to satellite underestimates of cloud

optical depth, likely caused by inhomogeneity within the satellite pixels. The overall agreement in the spatial variability and magnitudes of R_e and LWP demonstrates that the retrieval methods can be applied to mapping the distributions of these parameter fields for comparison with forecast model output.

3.2 COAMPS Model Implementation

COAMPS is a three-dimensional nonhydrostatic forecasting model developed at NRL (Hodur, 1997). The horizontal resolutions of the three nested domains used in this study are 81, 27 and 9 km. The bulk-water cloud microphysics scheme follows Rutledge and Hobbs (1983). Output data for the 9-km grid resolution are used in this analysis. The model was run twice daily using a 12 h data assimilation update cycle, so that each forecast was initialized using a first guess analysis from the previous 12 h forecast combined with current observational data using a multivariate optimum interpolation scheme. The data assimilation was continuous through the month of August 1999. A 36 h forecast was produced from the 0000 UTC run for flight planning purposes. The 1200 UTC run produced a 12 h forecast in order to maintain the data assimilation cycle.

The Rutledge and Hobbs (1983) scheme features five prognostic equations for the following species of water substance: water vapor, cloud water, rain water, cloud ice, and snow. Thirteen processes for conversion from one species to another are included. Of most interest in this study are conversions to and from water vapor and cloud water and the autoconversion of cloud water to rain water. The autoconversion threshold is fairly high, so that the model produces rain water only after attaining 1 g kg^{-1} liquid water mixing ratio and thus the model is unable to produce drizzle. The lack of this important sink of cloud water results in an over-prediction of liquid water content.

COAMPS does reproduce the observed strong cloud top cooling over a shallow layer due to longwave radiative flux divergence. The turbulence scheme responds to destabilization of the cloud top by producing large turbulence intensity, promoting entrainment and strengthening of the inversion. This tightly coupled, nonlinear interaction between clouds, radiation, and turbulence is critical in correctly modeling the evolution of marine stratus and stratocumulus (Oliver *et al.* 1978; Thompson *et al.* 1997). The COAMPS model was run in two modes; first using 30 vertical levels in the 'operational' mode as was carried out for the realtime forecasting during the field project; and then using 45 levels in 'high resolution' research mode, with 60 m vertical resolution in the lower levels (to 1600 m altitude).

The COAMPS model's sigma level data, and the output fields closest in time to the aircraft observing period, are used for analysis. In the cloud microphysics scheme, water substances are divided into four categories, cloud water, rain water, ice crystals and snow. For purposes of comparison to satellite and aircraft data, liquid water path was derived by vertical integration of cloud water mixing ratio greater than $10^{-7} \text{ kg kg}^{-1}$ between cloud base and cloud top, scaled for each layer from mixing ratio to liquid water content.

3.3 Case Study of 9-11 August 1999

Detailed analyses have been completed for several case studies including multi-day sequences. A three-day sequence of August 9-11 was selected due to the observed evolution of the boundary layer dynamic structure and cloudiness as well as the availability of simultaneous satellite and aircraft datasets. The synoptic pattern is characterized by a weak surface trough over the western U.S. and an offshore high to the northwest of the project area, with passage of a weak upper-level trough across the northern Oregon coastal region during August 10-11.

Model forecasts of the temperature and cloud liquid water content for 9-11 August are shown in Figure 8, using grid-point vertical profiles selected from the area of the aircraft sampling flights. The areas of aircraft flights are shown as graphic overlays on a sequence of visible satellite images from this period (Figure 9). During this three-day sequence, the COAMPS MBL deepens significantly and the cloud field transitions from scattered thin stratus to banded, cellular stratocumulus with very high cloud liquid water content. Examination of 3-hourly cross sections (not shown here) extending from the coast to 130W (~500 km distance) and from the surface to 3 km indicates that initially the MBL is 300-500 m deep with scattered clouds. The clouds become more extensive during the period and by 0000 UTC 10 August they span the entire cross section. The MBL begins to deepen rapidly at 30 hours as the cloud thickness increases. By 36 h (1200 UTC 10 August), the mean boundary layer depth is ~750 m and the cloud layer is uniformly 600 m in depth. The MBL continues to deepen over the next 12 hours while the cloud thickness decreases and inhomogeneities develop in the cloud liquid water content. By 48 hours (0000 UTC 11 August), the cloud layer is discontinuous with individual elements exhibiting vertical development, suggestive of a transition from stratus to stratocumulus. The inversion at the top of the MBL reaches an elevation of ~ 2 km with significant stratification in the upper part of the MBL both within the clouds and in clear areas between cloud elements.

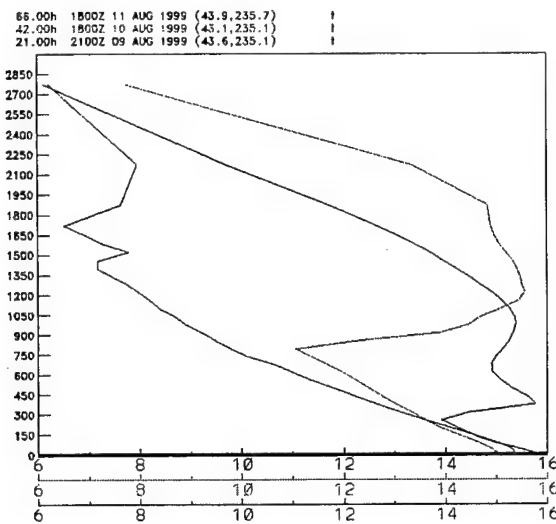


Fig. 8(a). COAMPS predicted profiles of temperature (deg C) on 9 August (black), 10 August (red) and 11 August (blue) for grid point profiles taken in the region of aircraft sampling.

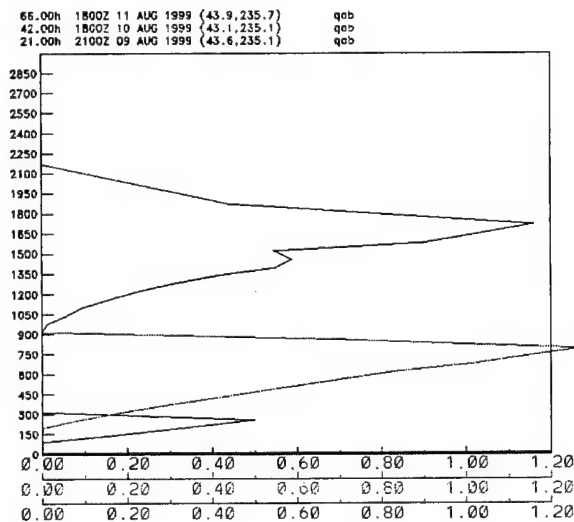


Fig. 8(b). COAMPS predicted profiles of cloud liquid content (LWC, g m⁻³) on 9 August (black), 10 August (red) and 11 August (blue) for grid point profiles taken in the region of aircraft sampling.

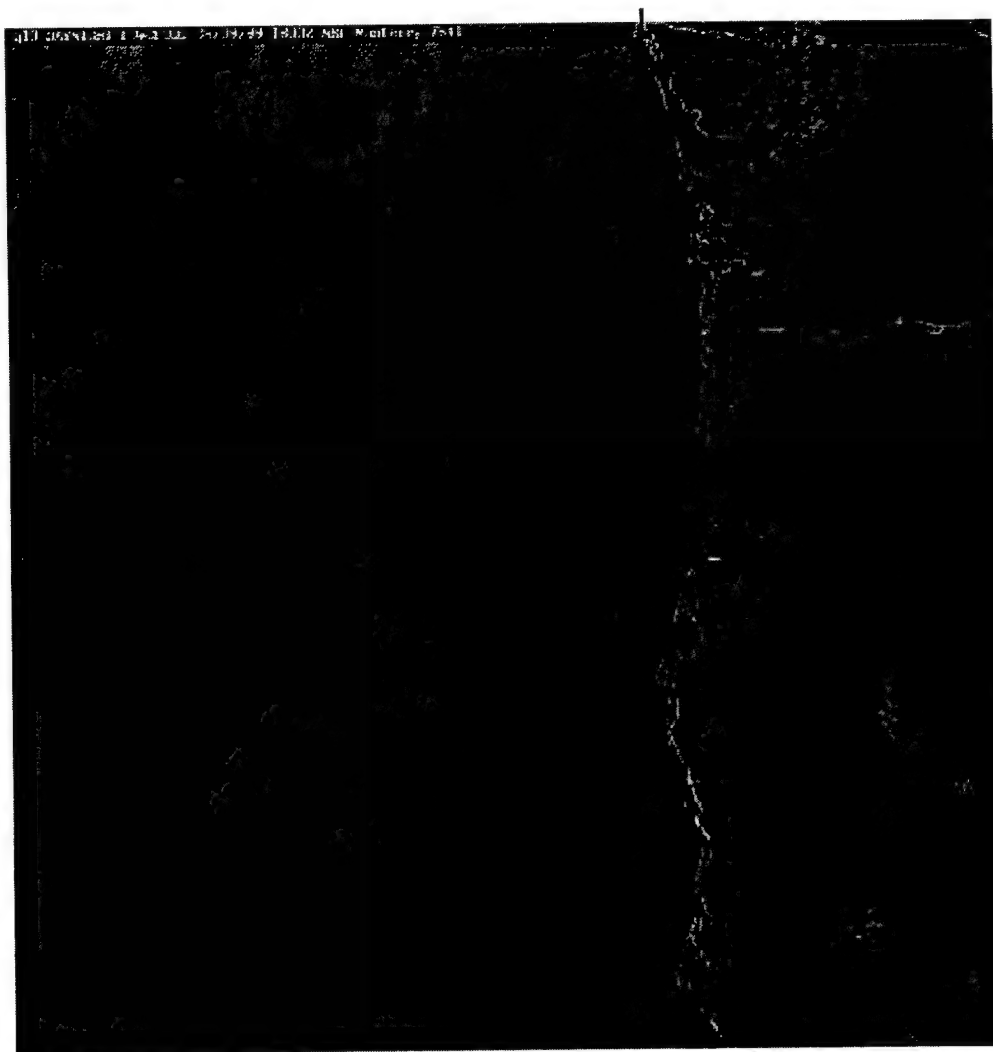


Fig. 9(a). GOES visible satellite image at 1800 UTC on 9 August 1999, with graphic overlay to indicate the general area of flight sampling.

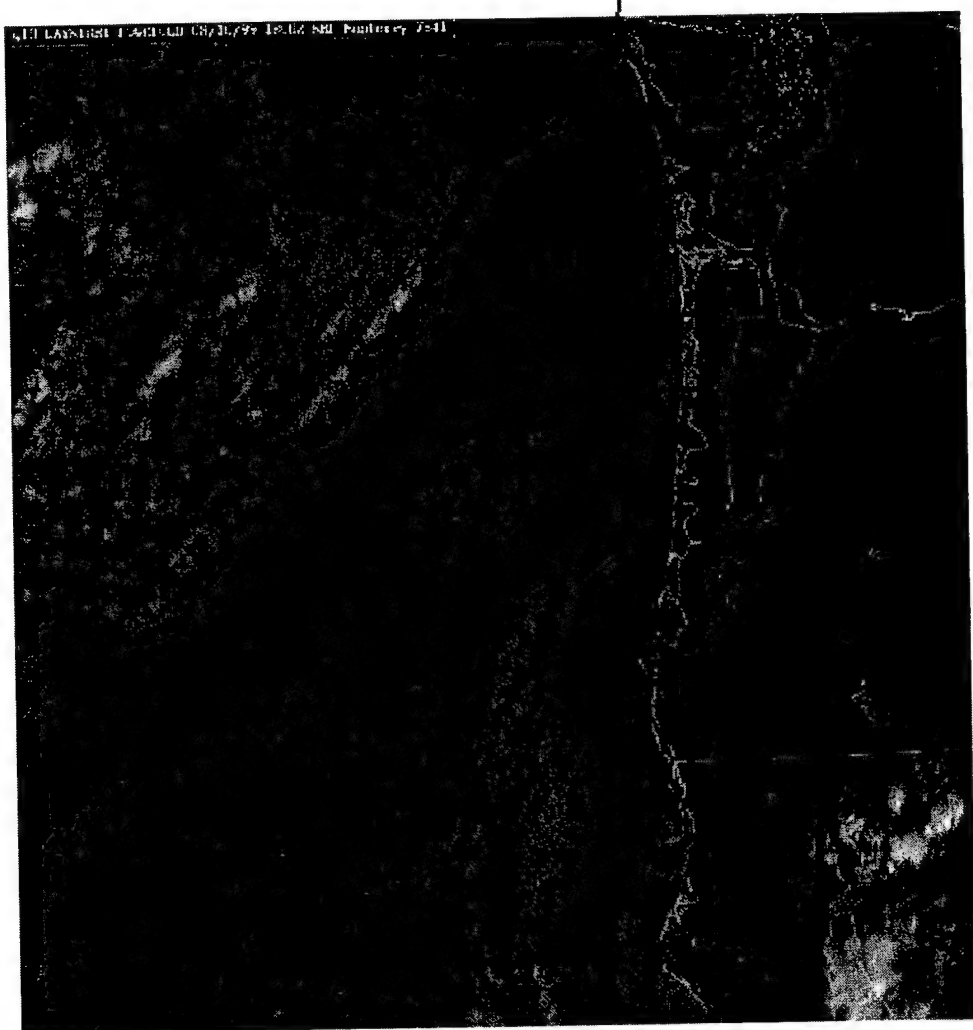


Fig. 9(b). GOES visible satellite image at 1800 UTC on 10 August 1999, with graphic overlay to indicate the general area of flight sampling.

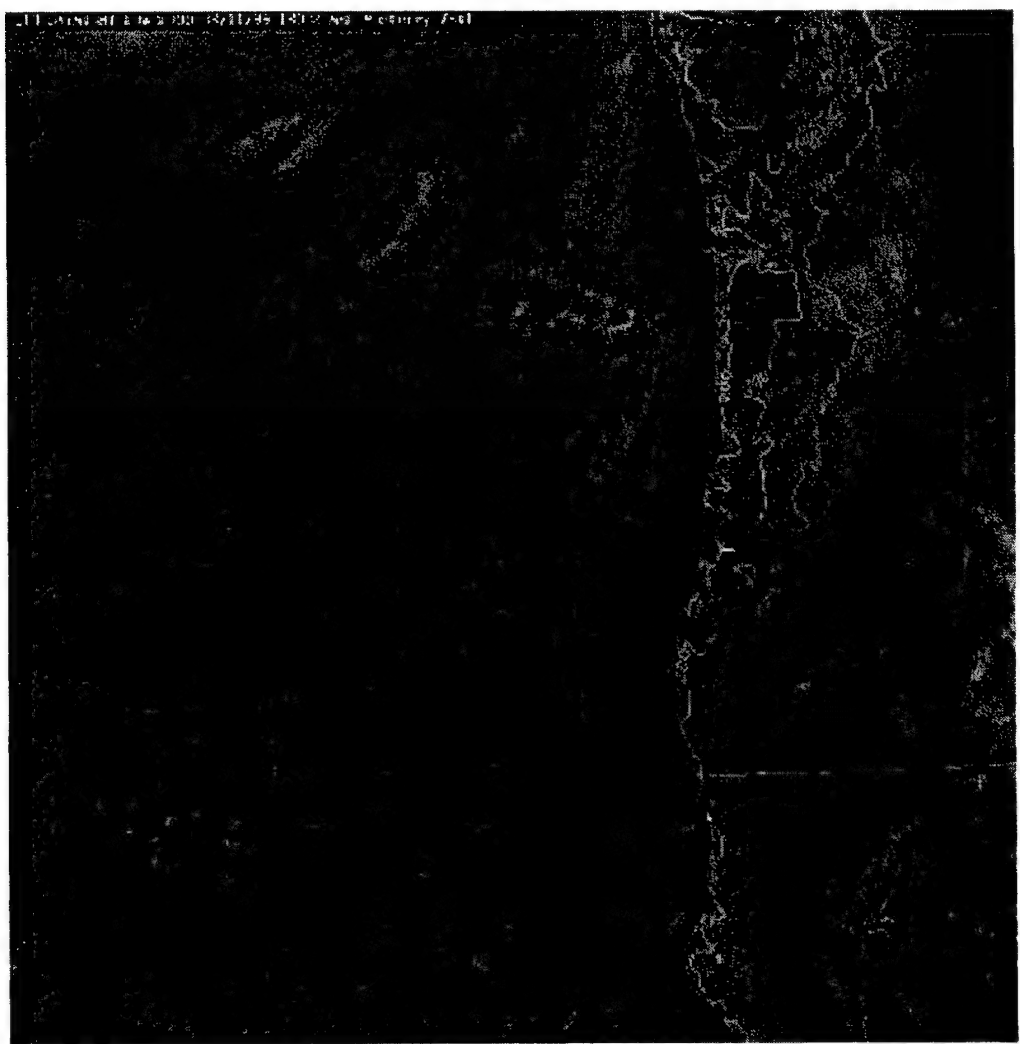


Fig. 9(c). GOES visible satellite image at 1800 UTC on 11 August 1999, with graphic overlay to indicate the general area of flight sampling.

Figure 10(a) shows the 18-hour forecast of vertically integrated cloud water path, valid at 18 UTC on 9 August. The maximum LWP values for the coastal cloud are in the range $0.1 - 0.2 \text{ kg m}^{-2}$. Figure 10(b) shows the model domain again, with an inset depicting the satellite-derived LWP. This sub-area is selected for detailed analysis of aircraft data for coastal cloud sampling. Maximum values of satellite-derived LWP are $0.05 - 0.1 \text{ kg m}^{-2}$ for this coincident time period. Also note the correspondence of the COAMPS-predicted cloud features along the north, south and west edges of the inset image.

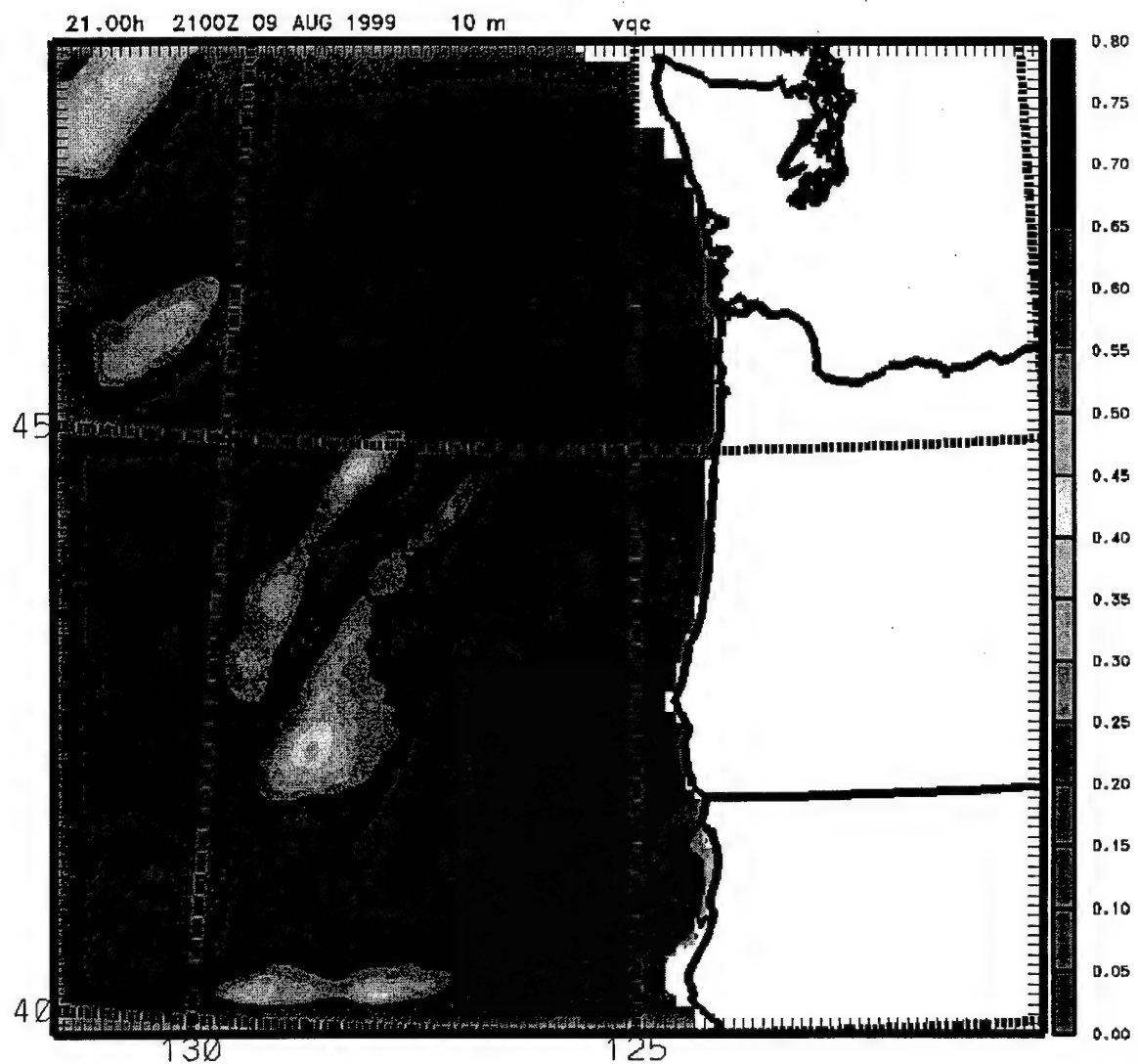


Fig. 10(a). COAMPS forecast of LWP (kg m^{-2}) for 2100 UTC on 9 August 1999.

fields were also re-analyzed into the same area map projection as the satellite-derived LWP gridded dataset (as shown in the inset of Fig. 10(b)). Fig. 12 and Fig. 13 present pairs of these corresponding LWP fields. Again, the similarity in the cloud field evolution can be seen between the satellite and model data. Also note the correspondence in the increasing extent of cloud field incursion onshore. However, notable differences occur in the magnitude of the maximum LWP values. The satellite-estimated LWP fields for the coastal cloud (Figure 12) reach a maximum of approximately 0.15 kg m^{-2} on 10 August, and 0.20 kg m^{-2} on 11 August. In contrast, the model-predicted LWP fields (Figure 13) indicate maximum values near 0.5 kg m^{-2} on 10 August, and exceeding 1.0 kg m^{-2} on 11 August.

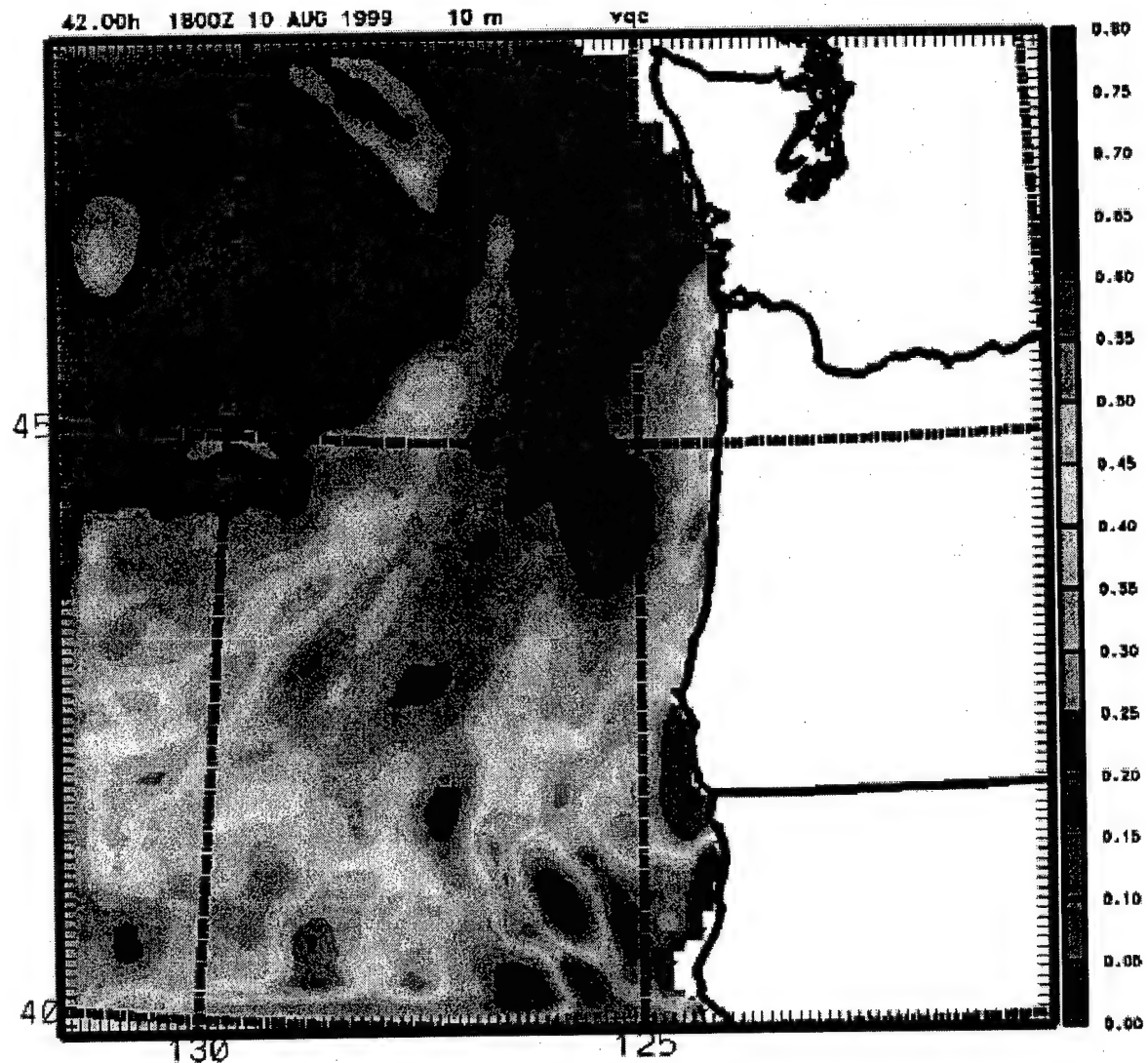


Fig. 11(a). COAMPS simulations of LWP at 18 UTC on 10 August.

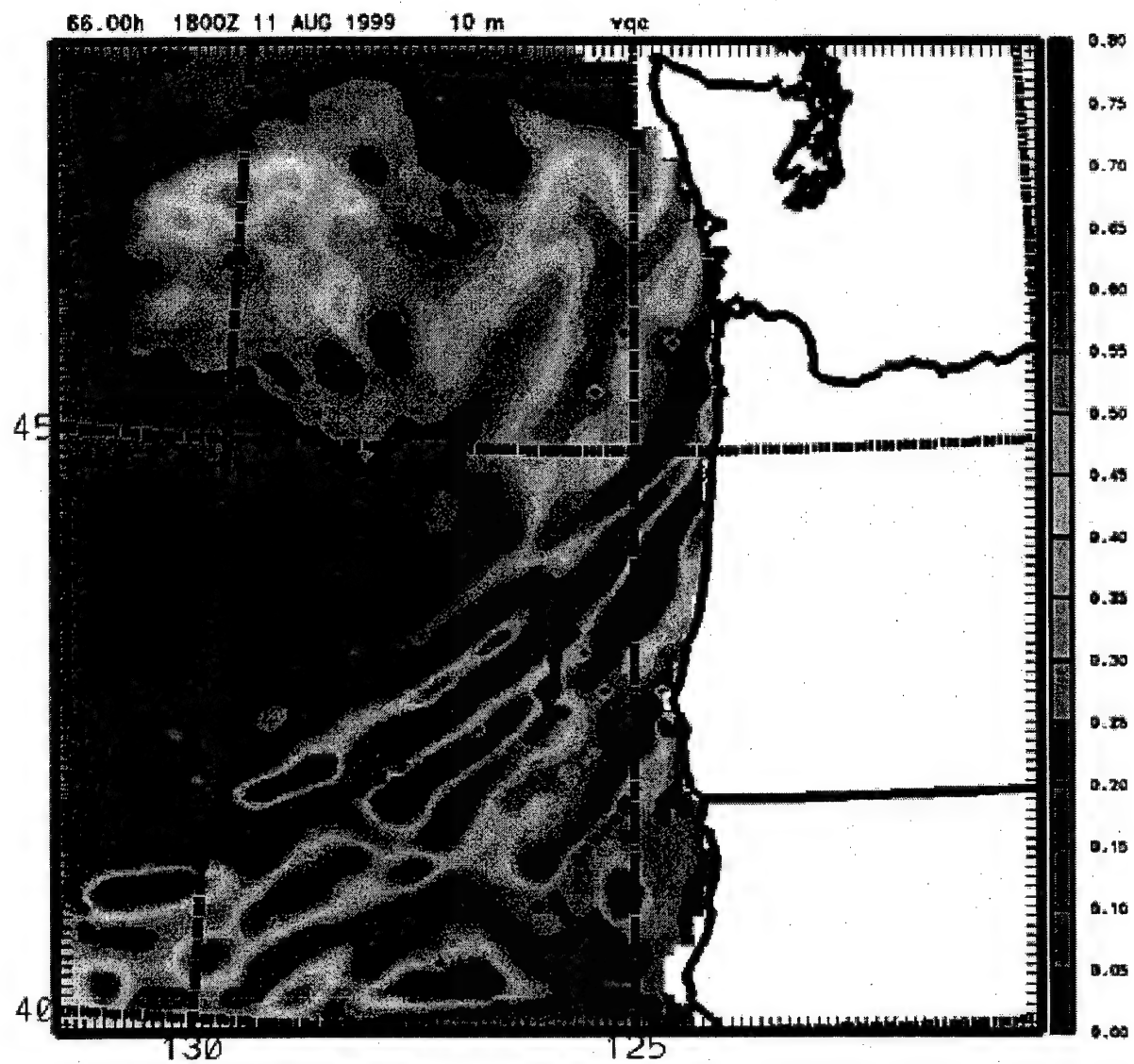
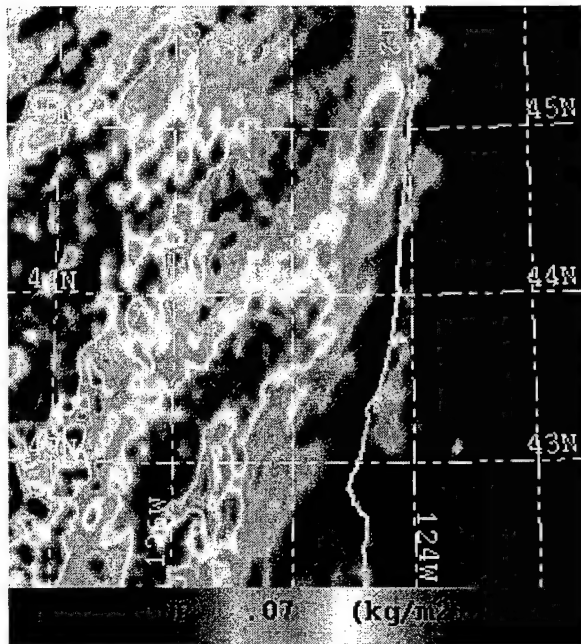
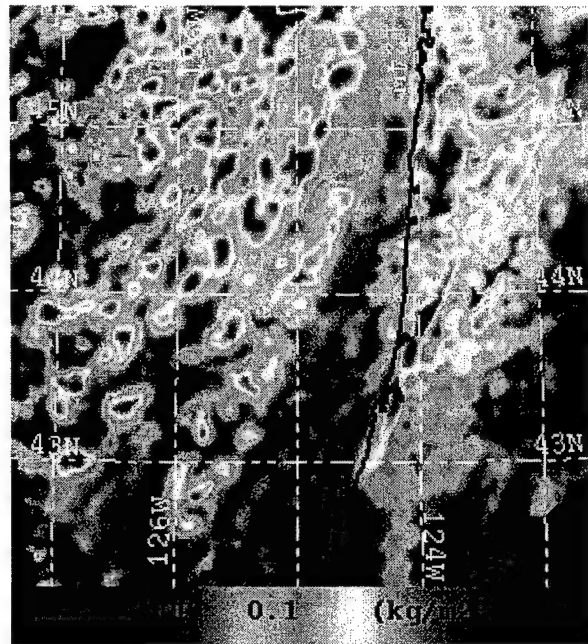


Fig. 11(b). COAMPS simulations of LWP at 18 UTC on 11 August.



(a)



(b)

Fig. 12. Satellite-estimated LWP at 18 UTC for (a) 10 August 1999 and (b) 11 August 1999, for the inset area shown in Fig. 10(b).

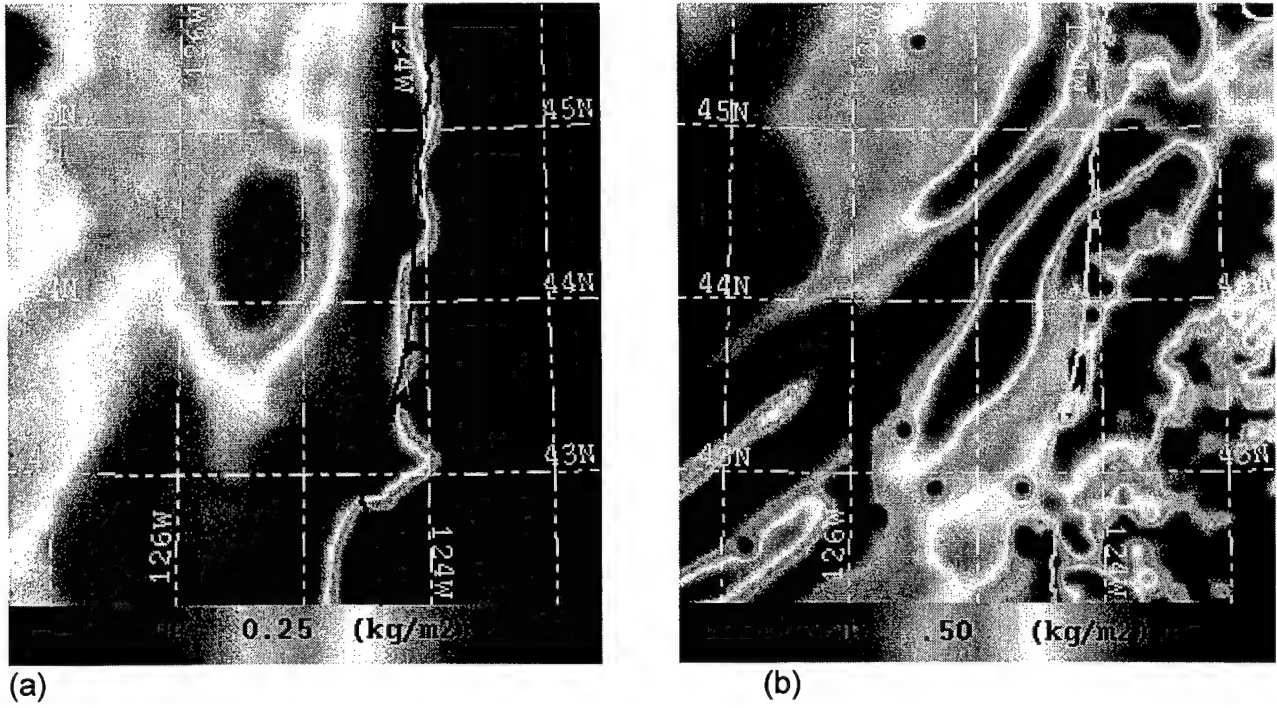


Fig. 13. Model-estimated LWP for 18 UTC on (a) 10 August 1999 and (b) 11 August 1999, corresponding to the area and map projection shown in Fig. 12(a) and Fig. 12(b).

Values of aircraft-estimated LWP for August 9-11 can be viewed in Table 1, but it should be noted that the values of LWP in this table are for specific short flight segments used in the satellite-aircraft comparisons, and do not represent the full range of values expected in the cloud field. A larger composite of aircraft measurements is presented in Figures 14-16, which portray the time-averaged mean and 90th percentile values of liquid water content as well as liquid water path for the sampling flights of August 9, 10 and 11. The values indicate agreement with the satellite estimates of LWP for Aug 9-11 as shown in Fig. 10(b), Fig. 12(a) and Fig. 12(b).

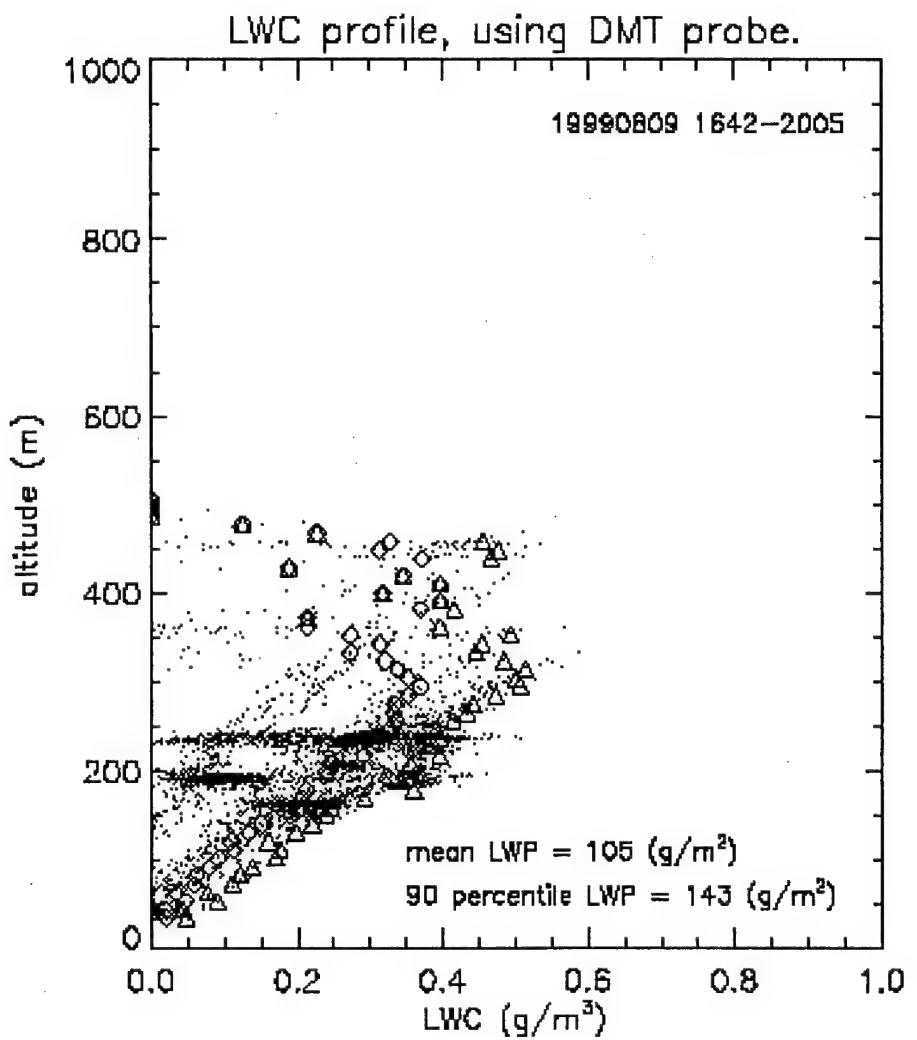


Fig. 14. Profile of LWC obtained from the entire flight of the King Air on 9 August 1999.

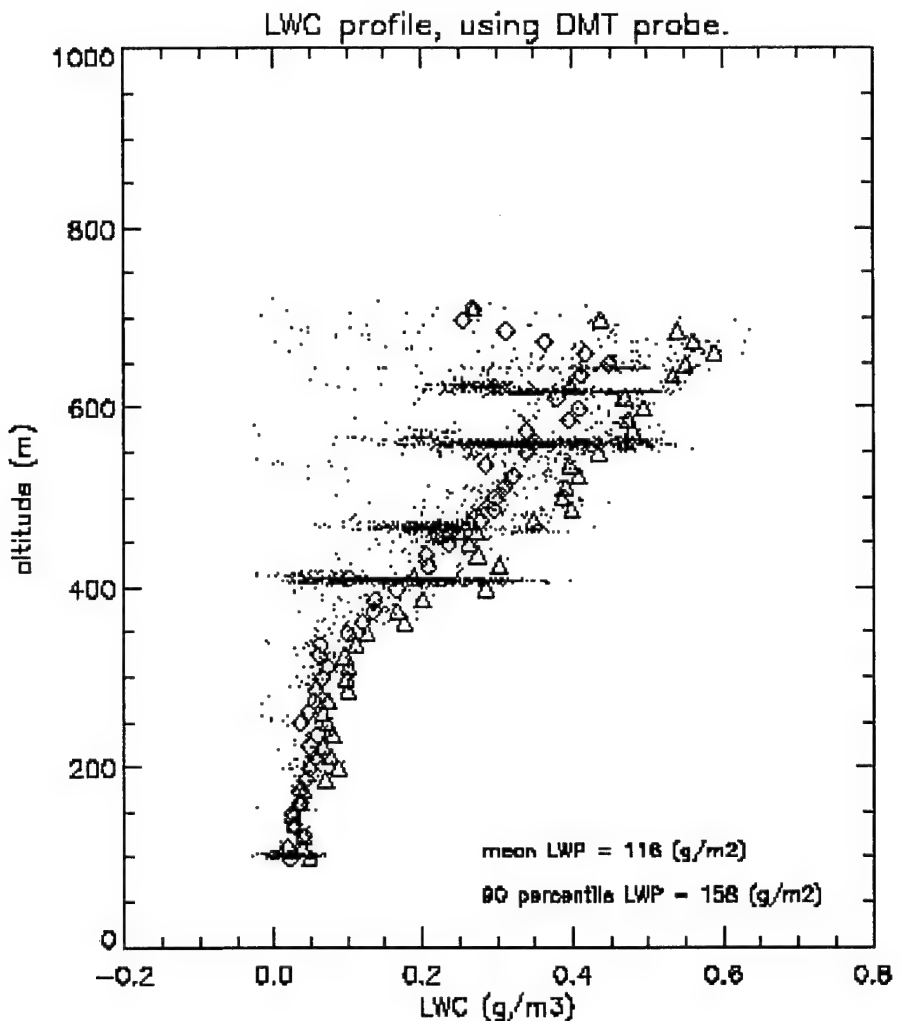


Fig. 15. Profile of LWC obtained from the entire flight of the King Air on 10 August 1999.

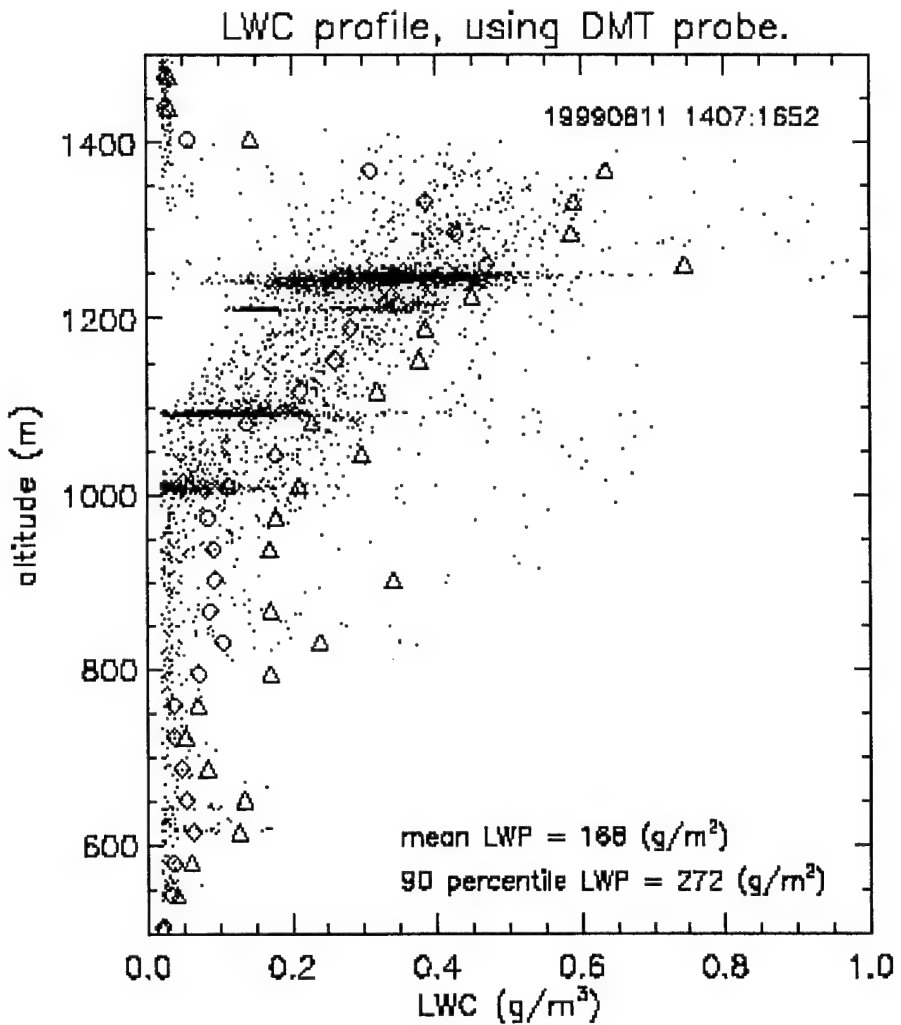


Fig. 16. Profile of LWC obtained from the entire flight of the King Air on 11 August 1999.

The aircraft data are temporal composites which include all cloud layers within the sampling period, including different zones of the cloud field, which combines deep and shallow cloud areas, so the composite aircraft LWP can be larger than most of the grid points in the satellite-derived LWP fields. Aircraft composite values of mean LWP are $104 - 140 \text{ g m}^{-2}$ for August 9, corresponding to maximum satellite LWP of 85 g m^{-2} ; on August 10 the aircraft values are $116 - 175 \text{ g m}^{-2}$, while satellite estimates are approximately 150 g m^{-2} ; on 11 August the aircraft LWP values ranged $152 - 177 \text{ g m}^{-2}$ while the satellite values reach approximately 200 g m^{-2} . Thus, the aircraft data confirm the trend and magnitudes in LWP as mapped from the satellite estimates, and indicate correspondence to the evolution of the cloud water vertical profiles predicted by the COAMPS (Fig. 8(b)).

The transition in cloud microphysical conditions was also evaluated by study of the variation in background average cloud condensation nuclei (CCN) and the corresponding mean cloud droplet concentrations over the three-day period. The CCN were sampled using a CCN counter (Vali *et al.* 1995) at 5 different supersaturation levels (0.2%-1%). The data represents a large amount of scatter on all three days, but clear trends can be deduced. When fit to the $N=C S^k$ form (where N is the CCN concentration, C is a constant representing the number of CCN at 1% supersaturation, S is the supersaturation and k is the slope parameter), the mean CCN spectra result on the three days of interest were $N=630 S^{1.4}$, $N=820 S^{0.45}$, and $N=320 S^{0.97}$, respectively. These values are subject to substantial errors, as the standard deviations at each supersaturation level were generally between 60-70% of the mean.

A comparison to the mean cloud droplet concentration on the three days (unfortunately number concentrations are missing on Aug 10 when the FSSP was lost) shows a general agreement with the trend and suggests effective supersaturations of approximately 0.3% on Aug 9 and 0.1% on Aug 11. The corresponding cloud droplet concentrations and their standard deviations are $139 \pm 37 \text{ cm}^{-3}$ on Aug 9, and $63 \pm 39 \text{ cm}^{-3}$ on Aug 11. Trends in CCN and cloud droplet concentration data suggest a transition to a cleaner maritime air mass on Aug 11.

The diagnosed overestimates in the model-predicted LWP may be caused by inadequate microphysical parameterizations of the model, such as the high threshold (1.0 g kg^{-1}) for autoconversion from cloud water to rain water (Kong, 1999). The mapped distributions of satellite-derived LWP indicate that modifications to model microphysical parameterization may be necessary. An experimental change in the autoconversion threshold was utilized to test the model sensitivity to this parameter. Figure 17 presents the 18 UTC forecast for 10 August, for a COAMPS simulation where the autoconversion threshold was reduced from 1 to 0.5 g kg^{-1} . This change in the threshold parameter caused a substantial reduction in the predicted LWP field. On the other hand, the model results indicated other undesirable effects of the parameter change, such as a vertical boundary layer profile with less similarity to the observed conditions. Thus, additional research is needed to investigate methods for representing the feedbacks between liquid water development, precipitation, and boundary layer convection.

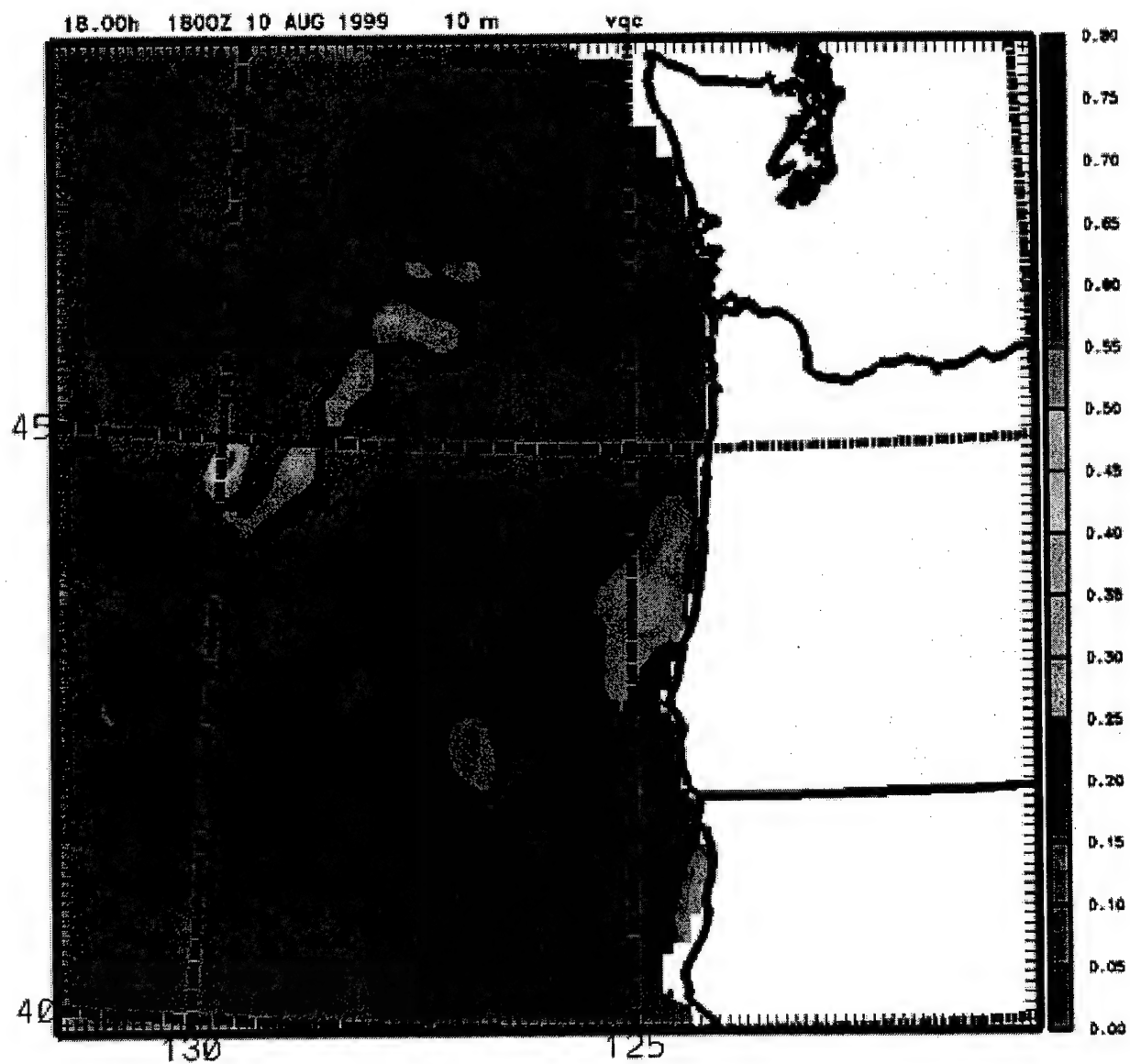


Fig. 17. COAMPS simulation of LWP at 18 UTC on 10 August as in Fig. 11(a), but for a change in the precipitation autoconversion threshold.

3.4 Additional Diagnostic Products

A variety of diagnostic procedures can be implemented by combining the satellite and model products for analysis of marine stratus, such as difference fields of model-satellite LWP. Temporal tendencies in satellite-observed parameters have also been mapped. The 2-hour tendency of LWP (Figure 18) indicates the location and magnitude of cloud layer evolution. Areas of increasing LWP during the morning hours help locate areas of enhanced updraft development and cellular structure, while areas of decreasing LWP such as that seen in the bay along the central coastline indicates erosion of the stratus cover. Tendency fields which indicate an increase in R_e could be used for short-term prediction of drizzle onset. The relationships between drizzle production, R_e and LWP are being studied using the aircraft microphysical and radar data from this experiment. Temporal changes in droplet size could also reveal local fluctuations in aerosol concentration.

Composites of parameters can be produced by averaging parameter values such as R_e at the same time on multiple days, for all days on which each pixel was cloudy and had a retrieved value of that parameter. Such climatologies of satellite-derived microphysical parameters can be extremely useful in classification of meteorological scenarios. For example, comparison of an R_e field with the "typical" climatology of cloud droplet size for a given time of day can be applied to model analysis and short-term forecasting of the subsequent cloud layer evolution.



Fig. 18. Temporal trend LWP (g m^{-2}) for 16-18 UTC, 9 August. Note the decreasing LWP (blue shading) over this two hour period (9-11 am LT) for the small bay (inland of white coastline, in lower portion of image), while LWP increases for the region a short distance offshore.

4.0 Summary

Analysis of case studies for coastal stratus offshore of Oregon has been used to demonstrate satellite remote sensing of cloud droplet effective radius (R_e) and liquid water path (LWP) for evaluation of mesoscale model forecasts. Intercomparisons of satellite-derived and aircraft datasets are used first to validate the satellite retrieval method for LWP. Secondly, the satellite, aircraft and COAMPS model intercomparisons reveal that there is very strong correspondence in the model 18-hour forecasts and satellite-observed cloud distribution and layer evolution, as well as in the three-day transition of the model-predicted and aircraft-observed cloud base and top heights. As the cloud layer evolves, however, COAMPS overpredicts the magnitude of cloud layer liquid water path, where maximum values of LWP are 3-4 times as large as those indicated from the observational data and mapped satellite estimates.

The model overprediction of LWP was somewhat reduced by increasing the number of vertical levels from 30 to 45, due to enhancement in the vertical grid resolution both within and above the boundary layer. Analysis of model-satellite LWP differences suggested the need for modifications of COAMPS current microphysical parameterization. A model experiment in which the liquid water autoconversion threshold was decreased from 1 to 0.5 g m^{-3} demonstrated further improvement in the magnitudes and horizontal distribution of predicted LWP.

It is not yet operationally feasible to operate the COAMPS model with 45 vertical levels at all times, so the satellite LWP fields could be used to identify situations where the higher vertical resolution is warranted on a temporary basis. The satellite retrieval methods can provide R_e and LWP fields with a spatial and temporal continuity, which is not available from other sources. Satellite-based analysis of these cloud parameters can also be used to create regional climatologies of cloud layer parameters, and to monitor cloud-aerosol interactions (Wetzel and Stowe, 1999). The overall results of the research just concluded support the rationale for assimilating remotely-sensed cloud liquid water path and perhaps even droplet size into COAMPS. Such assimilation can improve moisture initialization and cloud physics parameterizations at startup and during model runs. The field data from the COSAT '99 project was also used to test a new microphysical parameterization for COAMPS which has been developed at the University of Oklahoma. The results (provided by D. Mechem) demonstrate an improvement in the predicted cloud liquid water distribution, and point to an increasing need for satellite retrieval products for evaluation of the spatial distribution of predicted cloud field variables, particularly in remote regions where *in situ* measurements are not possible.

During the course of this research project, M. Wetzel initiated a collaborative project with Paul Tag and others at NRL-Monterey to implement the stratus microphysical retrievals for the NRL initiative on Data Fusion for Weather Assessment (DaFWA; Tag *et al.*, 2000). In addition, discussions with Tracy Haack and Steve Burk at NRL led new ideas on the potential use of satellite-retrieved parameters on the boundary layer thermodynamic profile for applications in atmospheric refractivity

mapping (Haack and Burk, 1999). Finally, we have suggested a cooperative observational and modeling effort with our NRL collaborators in conjunction with the upcoming DYCOMS-II field program in Summer 2001, which will focus on the structure and prediction of nocturnal stratus. These ideas have been incorporated into proposals for continued research in partnership with the NRL science teams.

5.0 References

Borys, R.D., D.L. Lowenthal, M.A. Wetzel, F. Herrera, A. Gonzalez, and J. Harris, 1998: Chemical and microphysical properties of marine stratiform cloud in the North Atlantic. *J. Geophys. Res.*, **103**, 22073-22085.

Greenwald, T.J., and S.A. Christopher, 2000: The GOES I-M Imagers: New tools for studying microphysical properties of boundary layer stratiform clouds. *Bull., Amer. Meteor. Soc.*, **81**, 2607-2619.

Haack, T. and S. D. Burk, 1999: Summertime marine refractivity conditions along coastal California. Third Conference on Coastal Atmospheric and Oceanic Prediction and Processes, New Orleans, 3-5 November, Amer. Meteor. Soc.

Hodur, R.M., 1997: The Naval Research Laboratory's Coupled Ocean/Atmosphere Mesoscale Prediction System (COAMPS). *Mon. Wea. Review*, **125**, 1414-1430.

Kong, F., 1999: A study of marine stratus and fog events using COAMPS model. *3rd Conf. on Coastal Prediction*, pp1-6, New Orleans, American Meteorological Society.

Lee, T.F., F. J. Turk, and K. Richardson, 1997: Stratus and fog products using GOES-8-9 3.9- μ m data. *Weather and Forecasting*, **12**, 664-677.

Mechem, D., Y. Kogan and F. Kong, 2000: A new microphysical parameterization for marine stratocumulus clouds in regional forecast models. *Proc., 13th International Conference on Clouds and Precipitation*, Reno, NV, 554-556.

Meier, W.N., J.A. Maslanik, J.R. Key, and C.W. Fowler, 1997: Multiparameter AVHRR-derived products for Arctic climate studies. *Earth Interactions*, **EI009**, 43 pp.

Minnis, P., P.W. Heck, D.F. Young, C.W. Fairall, and J.B. Snider, 1992: Stratocumulus cloud properties derived from simultaneous satellite and island-based instrumentation during FIRE. *J. Appl. Meteor.*, **31**, 317-339.

Oliver, D. A., W. S. Lewellen, and G. G. Williamson, 1978: The interaction between turbulent and radiative transport in the development of fog and low-level stratus. *J. Atmos. Sci.*, **35**, 301-316.

Platnick, and F. Valero, 1995: A validation of a satellite cloud retrieval during ASTEX. *J. Atmos. Sci.*, **52**, 2985-3001.

Rutledge, S.A. and P.V. Hobbs, 1983: The mesoscale and microscale structure and organization of clouds and precipitation in midlatitude cyclones. VIII: A model for the "seeder-feeder" process in warm-frontal rainbands. *J. Atmos. Sci.*, **40**, 1185-1206.

Stamnes, K., S.C. Tsay, W. Wiscombe and K. Jayaweera, 1988: Numerically stable algorithm for discrete-ordinate-method radiative transfer in scattering and emitting layered media. *Appl. Opt.*, **27**, 2502-2509.

Stephens, G.L., 1978: Radiation profiles in extended water clouds. II: Parameterization schemes. *J. Atmos. Sci.*, **35**, 2123-2132.

Tag, P.M., R.L. Bankert, M. Hadjimichael, A.P. Kuciauskas, W.T. Thompson and K.L. Richardson, 2000: Data Fusion for Weather Assessment (DaFWA) – An Application of Knowledge Discovery from Databases (KDD). *AIRIES '2000 Workshop on Artificial Intelligence Research in Environmental Science*, Annapolis MD, 13-15 November.

Thompson, W. T., S. D. Burk, and J. Rosenthal, 1997: An investigation of the Catalina Eddy. *Mon. Wea. Rev.*, **125**, 1135-1146.

Wetzel, M.A., and T.H. Vonder Haar, 1991: Theoretical development and sensitivity tests of a stratus cloud droplet size retrieval method for AVHRR-K/L/M. *Remote Sensing of Environment*, **36**, 105-119.

Wetzel, M.A., R.D. Borys, and L. Xu, 1996: Analysis methods for land-based fog droplet size and optical depth using satellite data. *J. Appl. Meteor.*, **35**, 810-829.

Wetzel, M.A., and L.L. Stowe, 1999: Satellite-observed patterns in stratus microphysics, aerosol optical thickness, and shortwave radiative forcing. *J. Geophys. Res.*, **104**, 31287-31299.

Wetzel M.A., S.K. Chai, M.J. Szumowski, W.T. Thompson, T. Haack, G. Vali, and R. Kelly, 2000a: Application of satellite microphysical retrievals for the analysis of the COAMPS mesoscale prediction model. *Proc., 13th International Conference on Clouds and Precipitation*, Reno, NV, 306-309.

Wetzel, M.A., W.T. Thompson, G. Vali, S.K. Chai, T. Haack, M.J. Szumowski, and R. Kelly, 2000b: Evaluation of COAMPS Forecasts of Coastal Stratus using Satellite Microphysical Retrievals and Aircraft Measurements, *Weather and Forecasting*, in review.

Vali, G., R.D. Kelly, A. Pazmany, and R.E. Macintosh, 1995: Airborne radar and in-situ observations of a shallow stratus with drizzle. *Atmos. Res.*, **38**, 361-380.

Vali, G., R. D. Kelly, J. French, S. Haimov, D. Leon, A. Pazmany, and R. E. McIntosh, 1998: Finescale structure and microphysics of coastal stratus. *J. Atmos. Sci.*, **55**, 3540-3564.

REPORT DOCUMENTATION PAGE

Form Approved
OMB No. 0704-0188

Public reporting burden for this collection of information is estimated to average 1 hour per response, including the time for reviewing instructions, searching existing data sources, gathering and maintaining the data needed, and completing and reviewing the collection of information. Send comments regarding this burden estimate or any other aspect of this collection of information, including suggestions for reducing this burden, to Washington Headquarters Services, Directorate for Information Operations and Reports, 1215 Jefferson Davis Highway, Suite 1204, Arlington, VA 22202-4302, and to the Office of Management and Budget, Paperwork Reduction Project (0704-0188), Washington, DC 20503.

1. AGENCY USE ONLY (Leave Blank)	2. REPORT DATE December 1, 2000	3. REPORT TYPE AND DATES COVERED Final: May 1, 1998 - October 31, 2000
4. TITLE AND SUBTITLE Forecast Model Applications of Satellite-derived Cloud Parameters		5. FUNDING NUMBERS G N00014-98-1-0556
6. AUTHORS Melanie A. Wetzel Steven K. Chai		
7. PERFORMING ORGANIZATION NAME(S) AND ADDRESS(ES) Desert Research Institute University & Community College System of Nevada 2215 Raggio Parkway Reno, NV 89512-1095		8. PERFORMING ORGANIZATION REPORT NUMBER N/A
9. SPONSORING / MONITORING AGENCY NAME(S) AND ADDRESS(ES) Office of Naval Research 800 North Quincy Street Ballston Tower One Arlington, VA 22217-5660		10. SPONSORING / MONITORING AGENCY REPORT NUMBER
11. SUPPLEMENTARY NOTES None		
12a. DISTRIBUTION / AVAILABILITY STATEMENT Unlimited		12b. DISTRIBUTION CODE
13. ABSTRACT (Maximum 200 words) Report attached.		
14. SUBJECT TERMS Clouds Satellite Micrometeorology		15. NUMBER OF PAGES 32
		16. PRICE CODE
17. SECURITY CLASSIFICATION OF REPORT Unclassified	18. SECURITY CLASSIFICATION OF THIS PAGE Unclassified	19. SECURITY CLASSIFICATION OF ABSTRACT Unclassified
		20. LIMITATION OF ABSTRACT

NSN 7540-01-280-5500

Standard Form 298 (Rev. 2-89)
Prescribed by ANSI Std. Z39-1
298-102